Electric Field Measurements around a Metal Oxide Surge Arrester

Spanias C.A., Christodoulou C.A., Gonos I.F., Stathopulos I.A.

High Voltage Laboratory, School of Electrical and Computer Engineering,
National Technical University of Athens, Greece

Email: christ_fth@yahoo.gr

Abstract - **Aim of the current work is the experimental study of the electric field distribution around a medium voltage metal oxide gapless polymeric housing surge arrester, since the study and the knowledge of the electric field around an arrester can be useful for diagnostic tests and design procedures. The measurements were carried out, using two appropriate calibrated field meters. The results are accompanied with their total uncertainties, which were computed using the obtained measurements and data from the calibrations certificates.**

I. INTRODUCTION

Surge arresters are semiconductor devices, which are used in electrical power systems in order to protect them against lightning and switching overvoltages. Arresters are installed between phase and earth and act as bypath for the overvoltage impulse, since they are designed to be insulators for nominal operating voltage, conducting at most few milliamperes of current and good conductors, when the voltage of the line exceeds design specifications to pass the energy of the overvoltage wave to the ground. Even though a great number of arresters, which are gapped arresters with resistors, made of SiC are still in use, the arresters installed today are almost all metal oxide arresters without gaps, which means arresters with resistors made of metal oxide [1]. The distinctive feature of a metal oxide arrester is its extremely nonlinear V–I characteristic, rendering unnecessary the disconnection of the resistors from the line through serial spark gaps, as it is found in the arresters with SiC resistors. Additionally, metal oxide arresters are inherently faster-acting than the gapped type, since there is no time delay due to series air gaps extinguishing the current [2].

The basic parts of a metal oxide surge arresters are the cylindrical metal-oxide resistor blocks, the insulating housing and the electrodes (Fig.1). Between the varistor column and the polymeric housing there is a glassfibre structure, that either completely encloses the resistor blocks or exerts sufficient force on the ends of the stack to hold the metal oxide blocks firmly together.

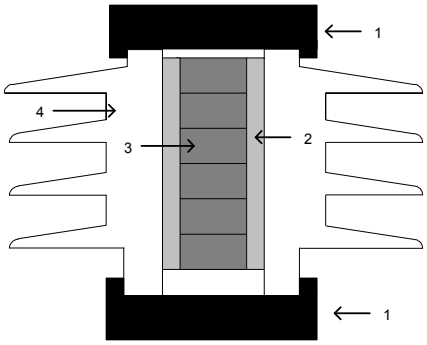

Figure 1 Metal oxide surge arrester cut
(1: electrodes, 2: fiberglass, 3: non linear resistor,
4: external insulator)

The electric field around a surge arrester is influenced by the geometry of the arrester and the electrical characteristics of the participating materials [3]. Electric field modelling helps the designers to know and consider the important factors affecting the maximum field intensity in the arrester, avoiding too high potential gradients inside and outside the arrester, especially during the transient conditions, a phenomenon which can cause damages to the arrester insulating system that brings it to a premature failure [4]. Hence, the study and the knowledge of the electric field around an arrester can be useful for diagnostic tests [5] and design procedures. Many researches have computed the electric field around a metal oxide arrester using appropriate simulation toolboxes (PC Opera, Cosmol, etc), examining different cases, such as surface pollution, broken sheds, etc [3, 4, 6-9]. Aim of this paper is the experimental study of the electric field distribution around a medium voltage metal oxide gapless polymeric (silicon rubber) housing surge arrester and the computation of the total uncertainty of the measurements.

II. MEASUREMENTS ARRANGEMENT

The test arrangement for the measurement of the electric field is shown in Fig. 2. The measurements were carried out in the High Voltage Laboratory of the National Technical University of Athens.

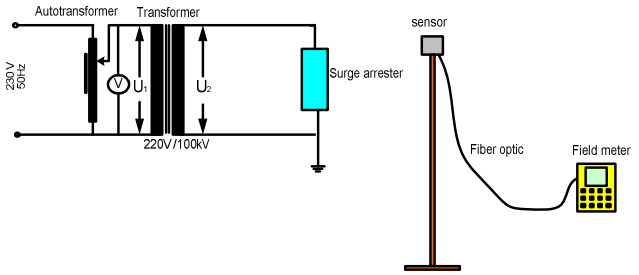

Figure 2 Experimental set-up used for the measurement of the electric field distribution.

Through a 230V/0…230V variac, a 220V/100kV transformer was fed. The voltage was measured in the primary of the transformer using a calibrated digital voltmeter. In order to measure the electric field around the surge arrester two appropriate calibrated field meters Narda and PMM / 8053. The sensors for each instrument, EFA 300 and EHP-50C correspondingly, are placed on an appropriate tripod and are connected via an optic fibber. Each one of both alternatively used sensors was moved in different directions:

a) on the horizontal plane, in various distances along three different axes (Fig. 3), and

b) in various heights.

For each point were taken repetitive measurements in order to evaluate the type A uncertainty. The user of the field meters stays at least 10m away from the sensor, otherwise interferences to the electric field and measurement accuracy may be caused.

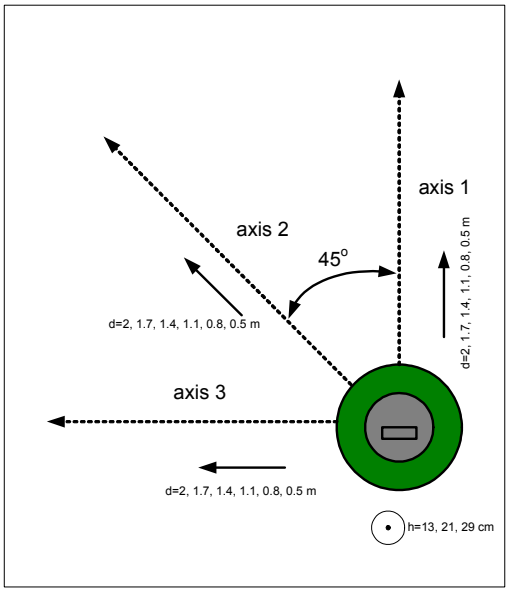

Figure 3 The three axes

III. UNCERTAINTIES' COMPUTATION

Uncertainty is a parameter characterizing the dispersion of the values attributed to a measured quantity. The uncertainty has a probabilistic basis and reflects incomplete knowledge of the quantity. All measurements are subject to uncertainty and a measured value is only complete if it is accompanied by a statement of the associated uncertainty. When a quantity is measured, the outcome depends on the measuring system, the measurement procedure, the skill of the operator, the environment, and other effects. Even if the quantity were to be measured several times, in the same way and in the same circumstances, a different measured value would in general be obtained each time, assuming that the measuring system has sufficient resolution to distinguish the values. Uncertainties are categorized in type A (or random uncertainty) and type B (or systematic uncertainty). Type A uncertainty u_r is computed with statistical analysis of series measurements, using equation (1):

$$u_r = \frac{ts_r}{\sqrt{n}} \quad (1)$$

where t is the Student's factor depended on the number of the measurements (n) for a given confidence level and s_r the standard deviation.

Type B uncertainty u_s is not evaluated statistically, but is estimated based on the uncertainty of the measuring system (stated in the calibration certificate), the drift in the value of the scale factor of the measuring system, the resolution of each instrument and the fact that the conditions during the use of a measuring system are different from those on the calibration (e.g. different temperature).

The derivation of the overall expanded uncertainty u is based on the square root of the sum of the squares of the systematic and random uncertainty contributions:

$$u = k\sqrt{u_r^2 + u_s^2} \quad (2)$$

where k is the coverage factor depended on the desired confidence level.

The type B uncertainty of the field meters is evaluated, using the calibration certificates, according to equation (3):

$$u_s = \sqrt{\Delta E_{READING}^2 + \Delta E_{CALIBRATION}^2 + \Delta E_{FIELD}^2} \quad (3)$$

where $\Delta E_{READING}$ is the contribution (rectangular) of the uncertainty of the reading

$\Delta E_{CALIBRATION}$ is the contribution (normal) of the uncertainty of the calibration

ΔE_{FIELD} is the contribution (rectangular) of the uncertainty of the non homogeneity of the field

The type B uncertainty of the Narda/EFA 300 field meter is calculated equal to 2.32% and of the PMM 8053 equal to 4.1%, for 50Hz and electric field range from 10V/m to 500V/m and 4.4% from 500V/m to 100kV/m.

IV. MEASUREMENTS RESULTS

Tables I-III present the measurements of the electric field for each position for the both instrumens, applying on the arrester voltage equal to 12kV, which corresponds to the nominal

value of a typical medium voltage power system of the Hellenic network.

Due to the fact that the arrester is not symmetrical, the measurements results are little different for the same h(cm) and d(m), dependent on the examined axis. The measurments were carried out for both Broandband (5Hz-2kHz) and Badpass (50Hz) cases, but there were not significant differrences, since there were not other electric fields in the laboratory and the input voltage had not harmonics. In Tables are presented the results for the Bandpass filter.

TABLE I ELECTRIC FIELD (V/M) AND UNCERTAINTY FOR THE THREE AXES, FOR BOTH THE FIELD METERS AND HEIGHT 130MM

h=13cm	Narda						PMM					
d	E_1	u_1	E_2	u_2	E_3	u_3	E_1^*	u_1^*	E_2^*	u_2^*	E_3^*	u_3^*
2	214.5	4.90	200.9	5.28	195.2	5.12	220.5	9.31	216.2	9.55	217.6	9.45
1.7	331	5.01	304.9	5.15	300.9	4.82	349.7	9.42	328.8	9.48	332.6	9.78
1.4	537.7	4.82	493.6	5.04	489.1	4.85	562.8	9.06	534.2	9.44	544.5	9.65
1.1	909.5	4.77	844.3	4.97	825.5	5.28	981.5	9.16	935.7	9.35	936.9	9.55
0.8	1663	5.02	1646	4.86	1625	5.07	1947	9.42	1833	9.66	1839	9.88
0.5	3803	5.11	3739	5.04	3726	5.02	4561	9.24	4276	9.89	4139	9.46

TABLE II ELECTRIC FIELD (V/M) AND UNCERTAINTY FOR THE THREE AXES. FOR BOTH THE FIELD METERS AND HEIGHT 210MM

h=21cm	Narda						PMM					
d	E_1	u_1	E_2	u_2	E_3	u_3	E_1^*	u_1^*	E_2^*	u_2^*	E_3^*	u_3^*
2	221.5	4.93	216.1	4.80	206.5	4.92	235.3	9.47	229.7	9.10	229.6	9.53
1.7	340.3	4.82	330.9	4.91	316.9	4.97	355.9	9.24	347.5	9.07	352.8	9.31
1.4	554.3	5.02	534.6	4.91	510.4	5.17	591.3	9.21	572.6	9.23	569.2	9.69
1.1	924.2	4.97	905.2	5.15	859.1	5.24	1017	9.08	995.8	9.24	986.2	9.15
0.8	1681	4.81	1702	4.92	1651	4.81	2031	9.54	1912	9.44	1879	9.50
0.5	3987	5.11	3991	5.03	3835	5.08	4696	9.64	4468	9.51	4421	9.38

TABLE III ELECTRIC FIELD (V/M) AND UNCERTAINTY FOR THE THREE AXES. FOR BOTH THE FIELD METERS AND HEIGHT 290MM

h=29cm	Narda						PMM					
d	E_1	u_1	E_2	u_2	E_3	u_3	E_1^*	u_1^*	E_2^*	u_2^*	E_3^*	u_3^*
2	224.4	5.01	221.5	5.03	213.5	4.69	253.2	9.31	250.9	9.42	257.4	9.24
1.7	342.4	4.95	336.2	5.02	323.5	5.023	383.8	9.20	390.4	9.53	393.2	9.33
1.4	566.1	4.79	540.5	5.06	523.1	5.081	619.5	9.44	632.4	9.40	632.1	9.55
1.1	960.3	4.75	911	4.94	869.9	4.91	1082	9.55	1086	9.35	1054	9.66
0.8	1740	5.09	1771	5.14	1653	4.76	2080	9.23	2067	9.69	2046	9.19
0.5	4050	4.95	4129	4.90	3981	4.84	4759	9.17	4659	9.44	4586	9.57

where d(m): the distance from the arrester on the horizontal axis

E_i (V/m): the electric field (V/m) for each axis i=1, 2, 3 for the Narda field meter

u_i (%): the total uncertainty the Narda field meter

E_i^*(V/m): the electric field (V/m) for each axis i=1, 2, 3 for the PMM field meter

u_i^* (%): the total uncertainty for the PMM field meter

Fig. 4 presents the electric field values of axis 1 for the Narda field meter in function with the height, including the calculated total uncertainties. The electric field increases approaching the high voltage electrode almost linearly.

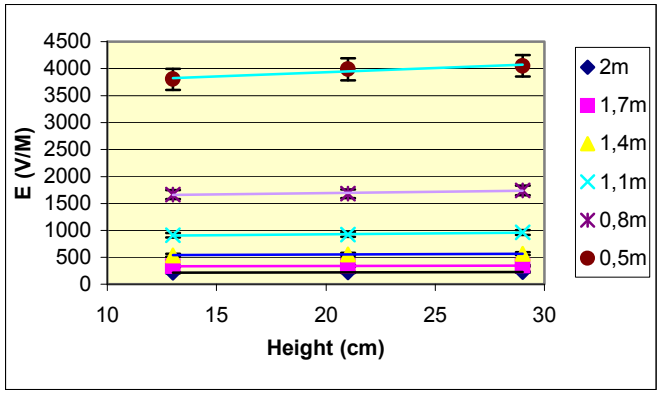

Figure 4 Electric field vs height
for the axis 1 using Narda field meter

Fig.5 shows the electric field variance in function with the distance from the arrester. The electric field reduces exponentially as the distance from the arrester increases.

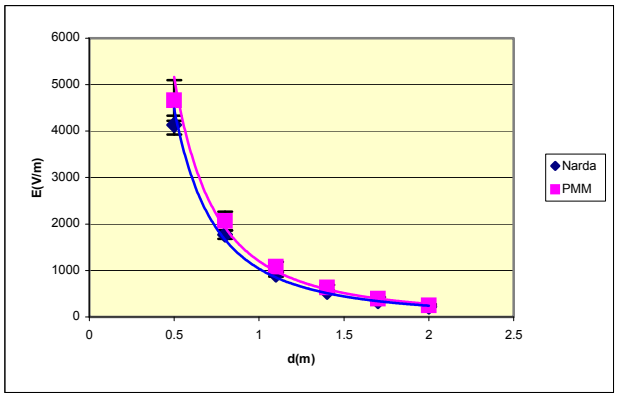

Figure 5 Electric field vs distance
for the axis 2 and height 29cm

Fig. 6 compares the electric field values obtained for both the instruments for the axis 3, 0.5 m away form the centre of the arrester. PMM gives in general higher values and uncertainties.

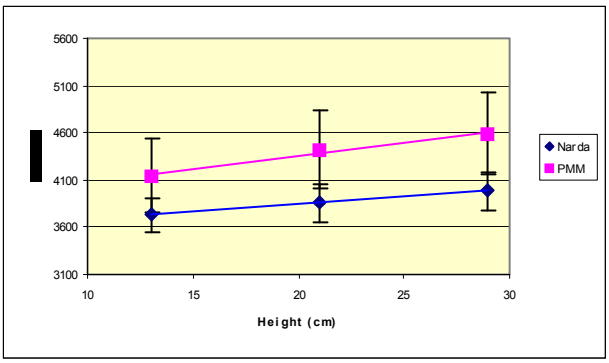

Figure 6 Electric field vs height
for the axis 3 and distance 0.5m

V. CONCLUSIONS

The current work presents measurements of the electric field around a medium voltage surge arrester for different heights, distance positions and axes. The knowledge of the electric field can be useful as an indicator for insulating system reliability of an arrester and can be useful for on line tests and design of new arresters. Two appropriate calibrated field meters were used and the measurement results are accompanied with their total uncertainty. Important role in the accuracy of the measurements play the position of the sensor, since the geometry of the arrester is unsymmetrical, the presence of metallic and grounded apparatus, the systematic uncertainty of each instrument and the steady supply of the high voltage. Future work includes measurements to damaged arresters and arresters with surface pollution and broken sheds and comparison of the measurements to simulated results obtained by Finite Element simulation program, in order to confirm that the designed in the program models represent adequately the behaviour of the arresters. Additionally, these models can be used for design changes decisions of the geometry and the materials of the arresters, in a way that the voltage distribution along the non-linear resistor and the electric field inside and outside the arrester to be uniform.

REFERENCES

[1] Hinrichsen V., 'Metal-oxide surge arresters. Fundamentals', (Siemens. 2001. 1st edn.)

[2] James R.E., SU. Q., 'Condition assessment of high voltage insulation in power system equipment' (IET Power and Energy Series 53. 2008. 1st edn.)

[3] B.Vahidi. R.Shariati Nasab. J.Sh. Moghani. S.A. Kashi. S.h. Hosseinian. 'Three Dimensional analyses of electric field and voltage distribution on ZnO surge arrester with broken Sheds', 2005 IEEe/PES Transmission and Distribution Conference & Exhibition: Asia and Pacific Dalian. China

[4] M. R. Meshkatoddini. ' Study of the Electric Field Intensity in Bushing Integrated ZnO surge arresters by means of Finite Element Analysis'. COSMOL Users Conference. 2006 Boston

[5] J.Lundquist. L.Stenstrom. A.Schei. B.Hansen. "New Method of the resistive leakage currents of metal-oxide surge arresters in service". IEEE Transactions on Power Delivery. Vol.5. No.4. November 1990. pp. 1811-1822

[6] B.Vahidi, R. Shariati Nasab, J.S. Moghani, "Analysis of Electric Field and Voltage Distributions on ZnO Surge Arrester for Polluted Condition", Proceedings of the XIVth International Symposium on High Voltage Engineering, Tsinghua university, Beijing, China, August 25-29, 2005

[7] F.Tighilt, A. Bayadi, 'Computed voltage distribtuinin ZnO arrester under pollutionby finite element method', 4th International Conference on Computer Integrated Manufacturing CIP'2007, 3-4 November 2007

[8] R. Karthik, 'A novel analysis of voltage distribution in zinc oxide arrester using finite element method', International Journal of Recent Trends in Engineering, Vol.1, No.4, May 2009, pp.1-3

[9] S. J. Han, J. Zou, S. Q. Gu, J. L. He, and J. S. Yuan, 'Calculation of the Potential Distribution of High Voltage Metal Oxide Arrester by Using an Improved Semi-Analytic Finite Element Method', IEEE TRANSACTIONS ON MAGNETICS, VOL. 41, NO. 5, MAY 2005, pp. 1392-1395

[10] IEC 60-2. 'High voltage test-techniques. Part 2: Measuring systems'. 1996-03